Defence Science Journal, Vol. 75, No. 1, January 2025, pp. 120-128, DOI : 10.14429/dsj.19326

The Degradation in Load Carrying Capability of Delaminated Specimens

Narendra Kumar Shrivastava[#,*], V. Suresh Babu[$], Manoj Kumar Buragohain[#] and Pushpam Dayal[#]

[#]DRDO-Advanced Systems Laboratory, Kanchanbagh, Hyderabad - 500 058, India
[$]National Institute of Technology, Warangal - 506 004, India
[*]E-mail: narendrashrivastava2010@gmail.com

ABSTRACT

Polymeric composites find extensive usage in aerospace applications, and their performance is influenced by environmental conditions throughout their life cycle. This study focuses on assessing the performance of composite laminates under different environmental conditions to evaluate the load carrying capacity (LCC) due to delamination. The laminates were specifically designed to withstand high pressure and temperature, ensuring satisfactory performance throughout their service life. The specimens, prepared according to ASTM standards with a thickness of 3 mm, featured different fibre orientations between the upper and lower laminates, including 0/0°, 0/30°, 0/45°, and 0/60°. The change in the delamination growth behavior for specimens subjected to different initial delamination lengths (a0) was studied using pre and post-radiographic tests (RT). The investigation encompassed a range of initial delamination lengths, from 70 mm to 110 mm, incremented by 10 mm. Notably, failure was observed in specimens with a 0/30º angle when the initial crack length (a0) reached 110 mm, while specimens with a 0/60º angle failed at an initial crack length of 80 mm. Additionally, it was noted that the maximum force required for the 0/30º angle laminate was observed when the initial crack length was 70 mm.

Keywords: Delamination; Double cantilever beam (DCB) specimen; Laminate; Mode-I; Load carrying capacity; VCCT

NOMENCLATURE

LCC	: Load carrying capacity
ASTM	: American society for testing and materials
RT	: Radiographic tests
a0	: Initial delamination lengths
DCB	: Double cantilever beam
MERS	: Modified epoxy resin system
VCCT	: Virtual crack closure technique
LEFM	: Linear elastic fracture mechanics
SERR	: Strain energy release rate
UT	: Ultrasonic testing
FEM	: Finite element method
CRMC	: Composite rocket motor casing
UD	: Unidirectional
UTM	: Universal testing machine
dB	: Decibel
SFD	: Source-to-film distance

1. INTRODUCTION

The use of metal is as old as civilization started. With the development of technology, we have shifted from metal to composites and used in various aerospace applications. The utilisation of composite materials has expanded from small-scale applications such as toys to more intricate components like aircraft, prosthetics for the human body, rockets, and other systems due to their lightweight nature and comparable mechanical properties to metals[1]. Consequently, scientists and engineers are keen on selecting an optimal blend of reinforcement and matrix materials to attain properties that precisely meet the specific structural requirements for a given purpose. The anticipated environmental conditions throughout various stages of the composite's life cycle greatly impact its performance. The failure of composite materials significantly diminishes their LCC. Failures can arise from different types of intralaminar fractures, including fibre breakage, microcrack development in the matrix, bonding issues between fibres and matrix, and delamination. Delamination, in particular, is a critical factor affecting the performance of composite materials[2]. During the manufacturing process, delamination occurs as voids between layers. These delamination defects, along with other manufacturing flaws, become embedded and can damage the composite structures during their service life. Delamination typically occurs at relatively low load levels, well before the full load capacity of the fibres is reached. As the presence and growth of such defects can adversely affect safety and durability, comprehending the impact of environmental conditions on the structural performance of composites is of utmost importance. This study focuses on identifying the reduction in LCC in laminates composed of T700 fibres with a Modified Epoxy Resin System (MERS) (LY556 & HY5200) (V_f=60 %). While a delaminated composite sample may experience a certain "mode" of failure initiation, the propagation and final failure modes can vary[3-5]. Three fundamental modes of interlaminar fracture are illustrated in Fig. 1.

Received : 31 July 2023, Revised : 28 April 2024
Accepted : 15 May 2024, Online published : 10 January 2025

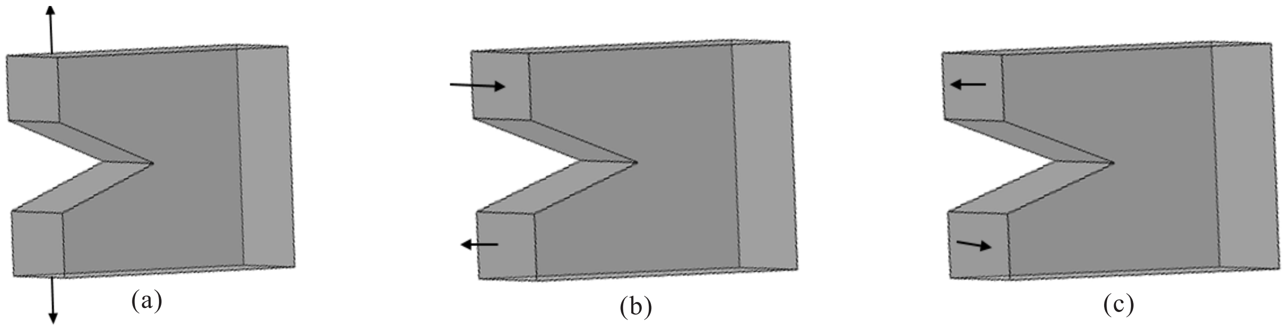

Figure 1. Basic diagram of (a) Mode I; (b) Mode II; and (c) Mode III.

Mode 1- The opening mode or peel mode
Mode II- The in-plane shear mode or sliding shear mode
Mode III -The out-of-plane shear mode or twisting shear mode

Delamination under tensile modes was investigated for T700 carbon fibre/ modified epoxy laminates under three-point bending using the virtual crack closure technique (VCCT) to measure the strain energy release rate (SERR)[6.] It is based on Linear Elastic Fracture Mechanics (LEFM). The energy released by a crack to grow its length from a to a+ Δa, must be the same to close the crack of length a + Δa to a. Experiments were conducted to find out the Mode I critical energy release rate (G_1C) at the interface of two laminate layups[7.]

2. LITERATURE REVIEW

However, composite structures are susceptible to the accumulation of damage. To ensure reliability, timely and accurate damage detection throughout the life cycle of a structure is critical. In this context, a comprehensive approach to laminate delamination detection using Ultrasonic Testing (UT) and transmission RT was developed. Although there have been many publications on the design, development, and qualification of composite materials over the past decade, there is a lack of comprehensive work on structural integrity assessment using the above-mentioned techniques. The purpose of this paper is to gain an in-depth understanding of delamination issues arising from process parameter variations during manufacturing and to conduct transmission detection using UT and RT. However, there are some challenges due to the lack of foolproof methods and reference standards in the open-source literature. To address this issue, custom reference laminates were fabricated to simulate defects such as delamination, different thicknesses, and layer sequence angles, and their ultrasonic response was characterised. The ultrasonic response of full-scale composites is also studied, and an overview for assessing the structural integrity of the samples is provided. Most studies focus on Finite Element Method (FEM) analysis or individual experimental evaluations. However, in this study, finite element analysis was first performed to experimentally verify the results[8.] The main goal is to achieve a close match between the finite element method and the analytical design so that the two sets of data verify each other and ensure that the design is safe and free of laminate failures. Therefore, this study was conducted at the subsystem level to simulate actual hardware configurations and experimentally evaluate the overall impact of delamination on MERS laminate performance in a comprehensive manner.

3. MATERIAL SELECTION

The manufacturing processes and materials used to make the laminates are similar to those used to make Composite Rocket Motor Casings (CRMCs). Carbon-epoxy and glass-epoxy composites are suitable candidates for filament-wound CRMC[9.] In this study, carbon fibre T-700 samples with MERS (LY556 and HY5200) (Vf = 60 %) were prepared by filament development and subsequent curing in the same way as CRMC, aiming to track and test various physical and Mechanical behaviour. Characterisation in the context of raw material properties and validation of design properties[10]. The coupons were fabricated using a wet filament winding process and tested on unidirectional (UD) laminates, as shown in Fig. 2 and Fig. 3, respectively. The cured samples were examined for resin content and density according to ASTM D3171 and ASTM D792, respectively. All mechanical testing was performed using a universal testing machine. (Instron UTM 4505). All test samples were dried in a dehumidification chamber and the moisture content was calculated. The first sample is weighed at ambient temperature, then dried and weighed again. Moisture content ≤0.1 % was observed. Tensile tests were performed on longitudinal specimens (Fig. 3) to determine the longitudinal tensile strength, modulus, and principal Poisson's ratio. Sample preparation and testing were performed in accordance with ASTM D3039 standards. To evaluate transverse tensile strength and transverse tensile modulus, tensile tests were performed on flat (90°) transverse directions specimens. The tensile modulus was determined by performing tensile testing on samples with 45° fibre orientation to determine the shear modulus (G12). The evaluated properties of Carbon T700/ Modified Epoxy composite are given in Table 1.

Figure 2. Winding of laminate.

Table 1. Properties evaluated for carbon T700/modified epoxy composite (V_f=60 %) from experimental result

Property	T 700 / Modified Epoxy resin composite
Longitudinal tensile strength, MPa	2000
Longitudinal tensile modulus. GPa	128
Poisson's ratio	0.29
Transverse tensile strength, MPa	14
Transverse tensile modulus, GPa	9.0
Longitudinal compressive strength, MPa	800
Transverse compressive strength, MPa	60

Table 2. Physical properties of cured composite – carbon fibre T-700 (LY556 & HY5200) (V_f=60 %)

Properties	ASTM Std. No.	Tested value
Tex, g/km	D 3800	804
Density, g/cc	D 3800	1.785
Filament diameter, micron	-	6.98
Tensile strength of Fibre, MPa	D 4018	4800
Tensile Modulus of Fibre, GPa	D 4018	225

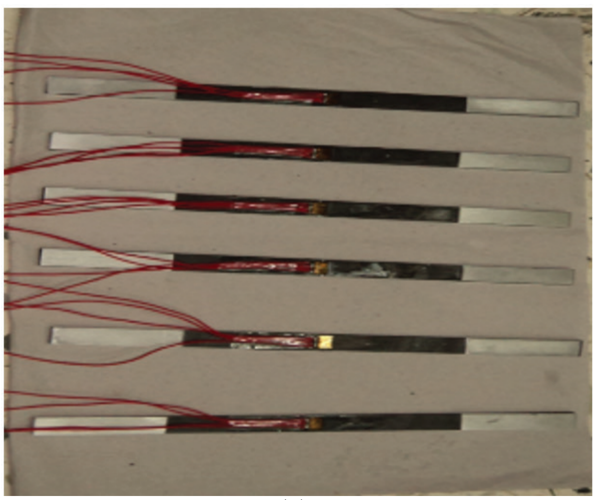

(a)

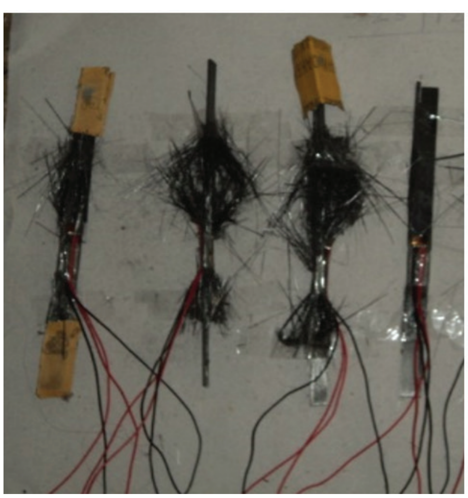

(b)

Figure 3. (a) Laminate with strain gauge; and (b) Failure modes of test results of composite (Vf = 60 %).

4. ANALYSIS ON MODE-1 DOUBLE CANTILEVER BEAM (DCB) SPECIMENS

FEM analysis was carried out to evaluate the damage tolerance capabilities, due to the different delamination topology. The crack was embedded inside the laminates and consequently, the crack area started to grow sy mmetrically with respect to the orthogonal axes, the length of the crack front increased accordingly. The following parameter can be changed in the macro element model to evaluate the effect of delamination:

- Delamination size[11]
- Ply sequence angle

4.1 FEM Flowchart

Tree diagram for FEM analysis is shown in Fig. 4. The laminate has a thickness of 1.5 mm, and delamination occurs between the 4th and 5th layers. To investigate the performance due to degradation of the laminate caused by delamination, 16 different pre-damaged (delaminated) models were created. These models specifically have delamination between the 4th and 5th layers. Initially, the ply sequence angle between the laminates was set at 0/0°, and the stress values were analysed by varying the initial delamination length. The initial delamination length starts at 70 mm and increases in increments of 10 mm until failure occurs. Furthermore, to analyse the impact of different ply sequence angles, four ply sequences were chosen: 0/0°, 0/30°, 0/45°, and 0/60°. The same methodology was repeated as 0/0° sequence[1]. For our study, we employed explicit finite element simulation using the APDL software. Initially, a 3D solid brick element with eight nodes (SOLID185) was selected, with the same properties as the T-700 with MERS carbon fibre, which were evaluated through an experiment (refer to Table 1 and Table 2). The software's INTER205 element was utilised to simulate the interface between two surfaces and the subsequent delamination process. Within the interface element, separation was depicted by a progressive

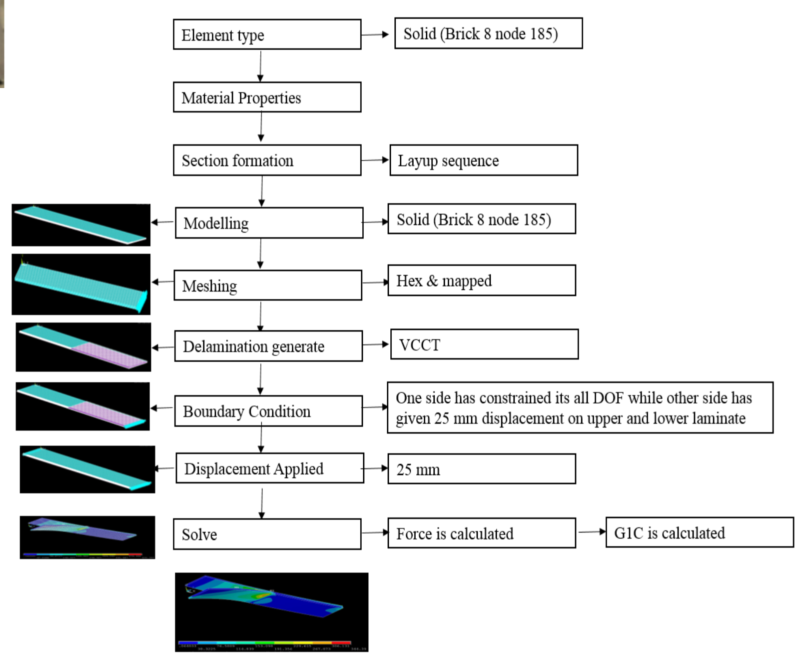

Figure 4. Algorithm of Mode I specimen for FEM.

displacement between nodes. All the relevant mechanical properties obtained from Table 1 were extensively used for the FEA. Cohesive elements were employed to describe delamination initiation and growth, aiding in capturing the intralaminar material behaviour of the composite. The VCCT approach was utilised for the delamination analysis. The FEM analysis model is depicted in Fig. 5.

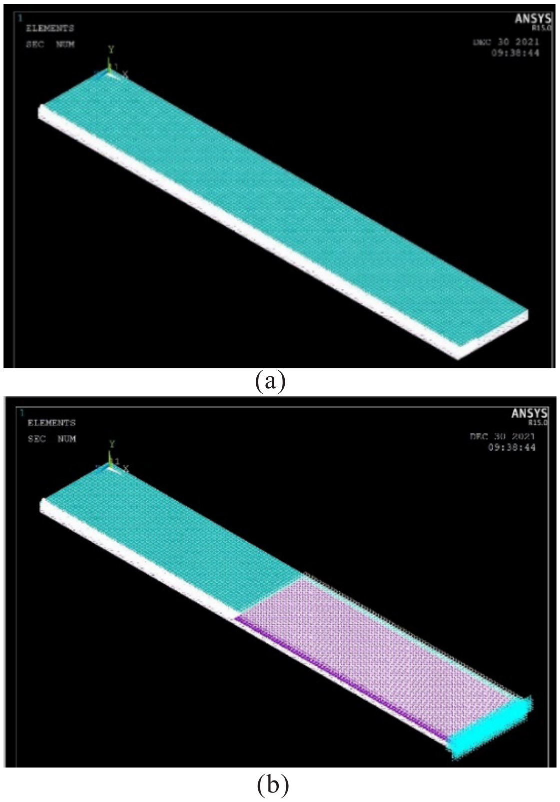

Figure 5. (a) Model with meshing; and (b) Model with various initial delamination length.

4.2 Modelling Setup

Sixteen different types of pre-damage models were created. To study the extended growth effect of the sample, initial cracks with different initial delamination lengths were found on the left, which occurred between layers 4 and layer 5, forming a cohesive zone. After the model is completed, meshing needs to be performed. Select "Hex" and "Mapping" as the meshing type.

4.3 Boundary Conditions

The analysis involves the use of a cantilever configuration for the composite panels, where one end is fixed and dynamic displacement constraints are applied to the other end. This configuration is shown in Fig. 6. The boundary conditions are:

- One side is fixed (all degrees of freedom are fixed)
- On the other hand, displacements were applied to the bottom and top laminates (initial displacement limited to 25 mm).

Figure 6. Boundary conditions and displacement at left end side.

4.4 Analysis Results

Load v/s displacement diagrams were recorded for 3 mm thick hybrid laminates at different layer sequences and different initial crack lengths in mode I, as shown in Fig. 7.

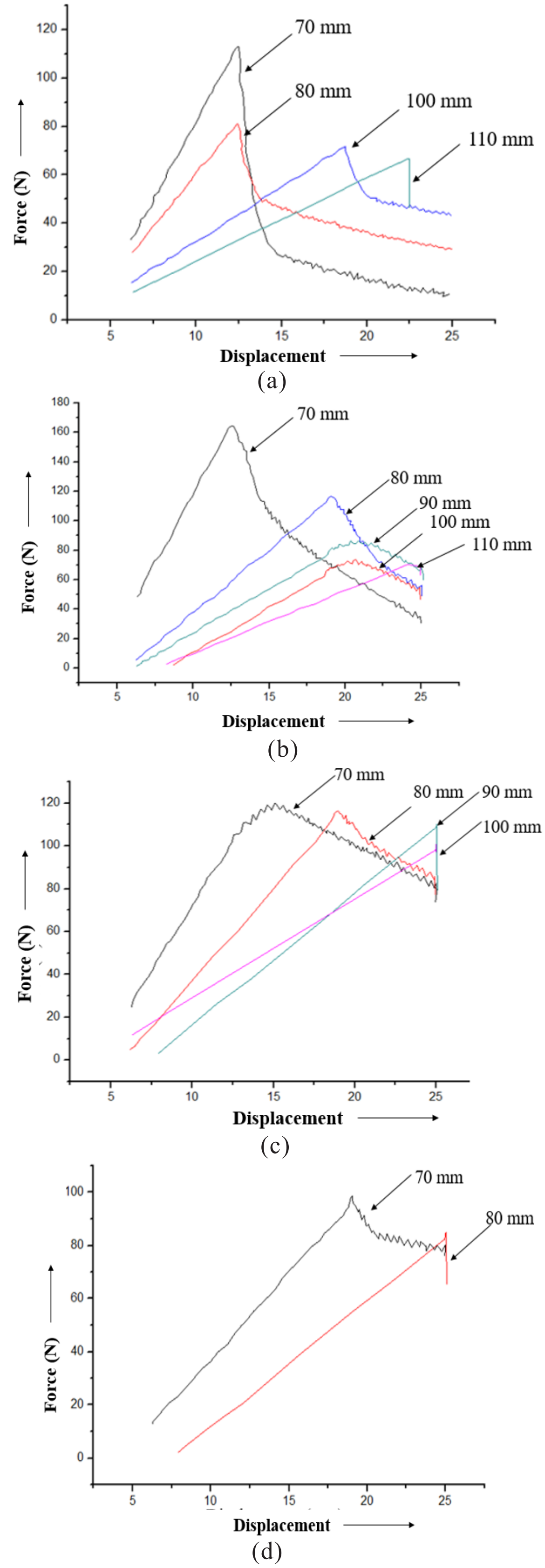

Figure 7. Force v/s displacement curve (a) 0/0°; (b) 0/30°; (c) 0/45°; and (d) 0/60° between upper and lower laminate.

Table 3. Theory used for evaluation of G1C

Theory	Formula	Parameter
Beam theory	$GIC = \frac{3Pc\delta}{2ba}$	
Modified beam theory	$GIC = \frac{3Pc\delta}{2b(a+\Delta)}$	Where, Δ = x-intercept of $C^{1/3}$ vs a compliance
Calibration method	$GIC = \frac{nPc\delta}{2ba}$	Where, n= slope of log(C) vs log(a)
Modified compliance calibration method	$GIC = \frac{3Pc^2\delta^{\frac{2}{3}}}{2A_1bh}$	Where, A_1 = slope of a/2h vs $C^{1/3}$; h = specimen thickness (mm)

The specimens exhibit a steep linear increase in the curves until a certain point, at which they abruptly fail, leading to a nonlinear decrease in the applied force. Figure 7 illustrates that the failure behaviour of the laminate varies in each case. As the angle between laminates increases, the peak values of force required for failure decrease, and this reduction occurs at a shorter initial crack length, which was crucial for calculating G1C. For instance, in the case of a 0/30º angle, the laminate fails after an initial crack length (a0) of 120 mm, while for a 0/60º angle, the failure occurs at just 80 mm of initial crack length. Similarly, increasing the initial crack length results in decreased force required for failure, but it also leads to greater displacement for a valid G1C determination. The FEM results are depicted in Fig. 8. In our study, various theories were employed to evaluate G1C, as outlined in Table 3. The evaluated values of G1C through FEM analysis are presented in Table 4.

Table 4. G1C evaluated value through FEM

Angle	a_o (mm)	P_c (N) (Max)	G1C value using Beam Theory (J/m²) (Avg)	G1C value using Modified Beam theory (J/m²) (Avg)	G1C value using Compliance calibration method (J/m²) (Avg)	G1C value using modified compliance calibration method (J/m²) (Avg)
0/0°	70	113.85	1219.82	1222.23	1220.32	1221.56
	80	81.168	760.95	763.42	758.32	765.37
	90	75.26	928.20	935.67	933.42	934.24
	100	71.22	799.3147	805.24	807.51	807.68
	110	61.48	753.521	742.35	743.12	748.32
0/30°	70	163.012	1746.01	1751.69	1748.96	1750.61
	80	116	1660.09	1666.34	1658.48	1664.18
	90	86.54	1198.291	1195.04	1199.64	1124.86
	100	73.67	914.69	919.84	910.25	912.54
	110	70.53	928.69	925.63	928.68	927.95
0/45°	70	120.966	1564.714	1574.35	1570.19	1572.43
	80	111.735	1647.197	1651.35	1654.73	1657.28
	90	110.397	1839.95	1836.21	1841.55	1843.61
	100	100.731	1510.965	1517.89	1521	1526.44
0/60°	70	98.82	1613.813	1612.52	1615.78	1614.2
	80	85.616	1642.814	1638.75	1640.85	1638.85

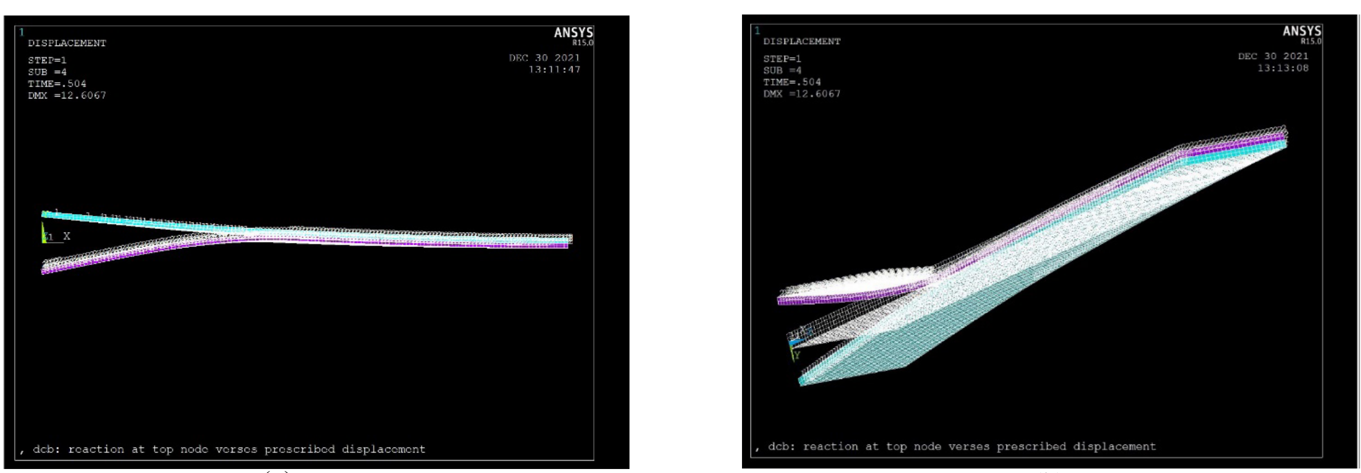

(a) (b)

Figure 8. For a0= 80 mm (a) Deformed shape; and (b) Deformed shape with un-deformed shape.

5. EXPERIMENTAL EVALUATION

5.1 Test Setup & Methodology

In this study, we fabricated test laminates with the same orientation and initial crack length used in the FEM analysis. The dimensions of each test sample are 200 mm long, 25 mm wide and 3 mm thick. The fibre orientations selected for the test samples matched those of the FEM analysis, which included 0/0°, 0/30°, 0/45°, and 0/60° angles. For experimental purposes, a pre-crack was introduced at the tip between the bottom laminate and the top laminate. Additionally, an additional 50 mm pre-crack was fabricated to accommodate the 50 mm long bracket, allowing the UTM to exert forces similar to the FEM analysis setup. The midplane of each sample contained polytetrafluoroethylene inserts of varying lengths that acted as delamination initiators. The flat test specimen is produced using a filament winding process, as shown in Fig. 9. The process involves wrapping the UD matrix around a large mandrel, cutting and removing the wrapped material from the mandrel, then laying the material flat, setting and curing in an autoclave. The carbon fibres are impregnated using filament winding technology by heating the resin system to 45 °C. After the filaments are developed, the laminate undergoes a curing process in an oven with precisely controlled temperatures. The flat mandrel is placed in the oven and supported by a metal stand. Table 5 provides details of the cure cycle.

(a)

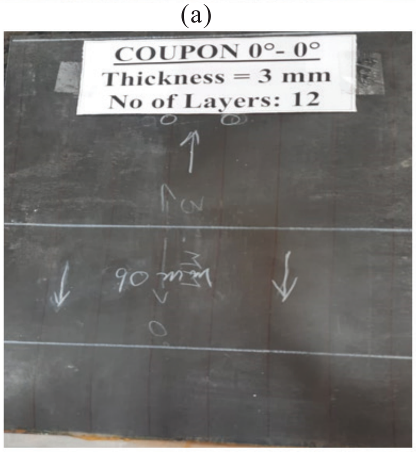

(b)

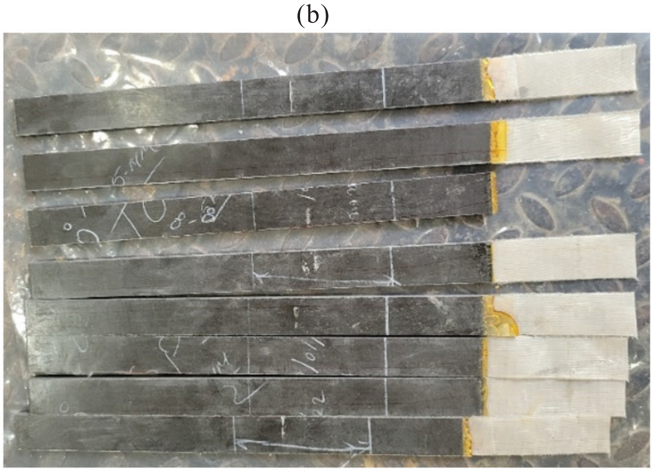

(c)

Figure 9. (a) During filament winding; (b) Coupon prepared; and (c) Coupon with teflon sheet coupons.

Table 5. Cure cycle

Initial temperature (°C)	Final temperature (°C)	Time (min.)	Remarks (heating rate per minute)
Room temperature	120	30	2 to 4 °C
Hold at 120° C		180	
120	160	30	2 to 4 °C
Hold at 160° C		180	
Switch off the oven and allow the component to cool naturally.			
Open the door and remove mandrel when it is below 40 °C.			

Delamination is detected and confirmed using Non-Destructive evaluation techniques such as radiographic imaging. RT was carried out for each specimen and found to be as predicted. Radiographic image for 0/30° having 70 mm initial crack length as shown in Fig. 10. To precisely identify the type of discontinuity present, we correlated areas of high decibel (dB) loss with tangential X-ray radiography images. The X-ray radiography was conducted in regions exhibiting significant dB loss using a 4MeV LINAC machine.

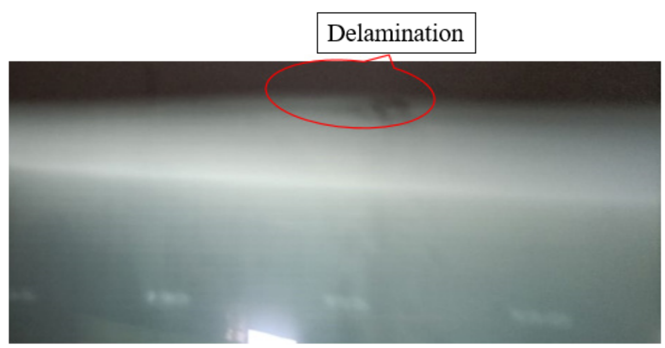

(a)

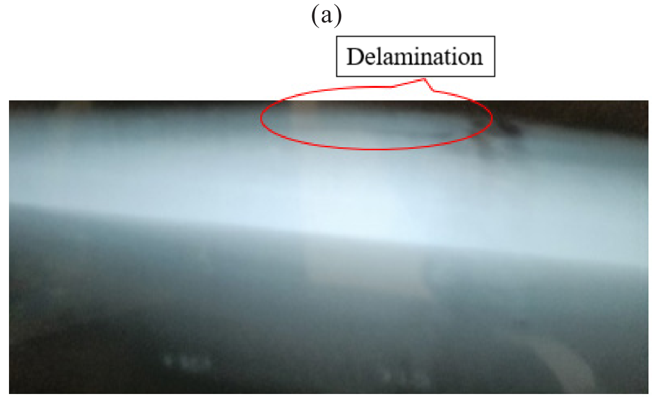

(b)

Figure 10. Delamination (a) Before the experiment; and (b) After the experiment.

We opted for a source-to-film distance (SFD) of four meters and an exposure time ranging from one to two minutes for the examination. In Fig. 10, we depict radiographic images capturing the high dB loss zones. Zones exhibiting a dB loss greater than 12 have been determined to indicate delamination. In essence, we characterized and analysed the high dB zones, identifying their nature and extent relative to the overall inspected area, shedding light on potential structural issues such as delamination.

Use a band saw to cut the laminate in different directions. Assemble the load application system and place the plate in the machine's handle and secure by adjusting first the lower hinge and then the upper hinge to fully level. The samples were loaded with UTM in displacement-controlled mode at a loading rate of 0.5 mm/min following ASTM standard D 6671/D 6671M-06. The experimental test setup and camera setup are shown in Fig. 12 and Fig. 13 respectively. A custom-made loading system was used to accurately measure the load applied during the experiment as well as the extent and propagation of the crack front. These measurements were recorded numerically and visually as shown in Fig. 13. Displacements were measured throughout the experiment and by crosshead movement of the UTM.

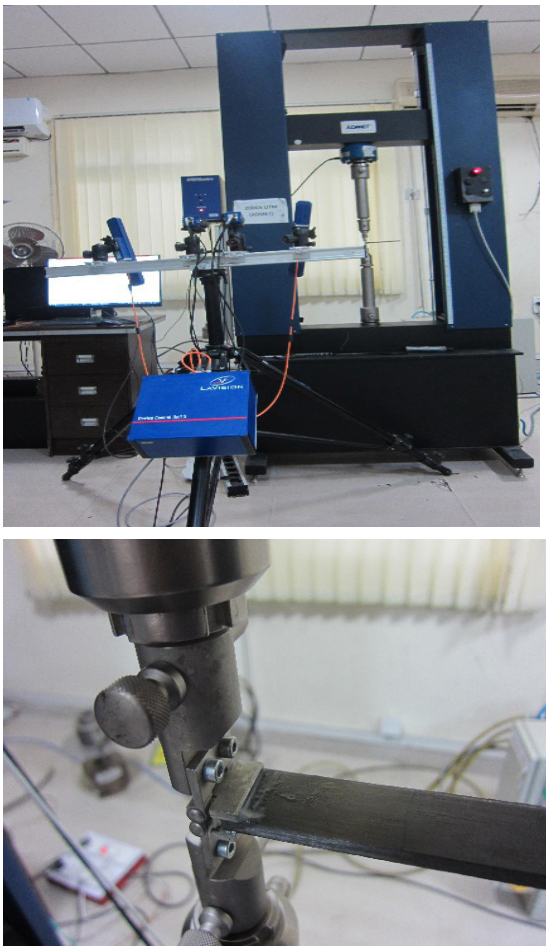

Figure 11. Test setup.

Figure 12. Camera setup.

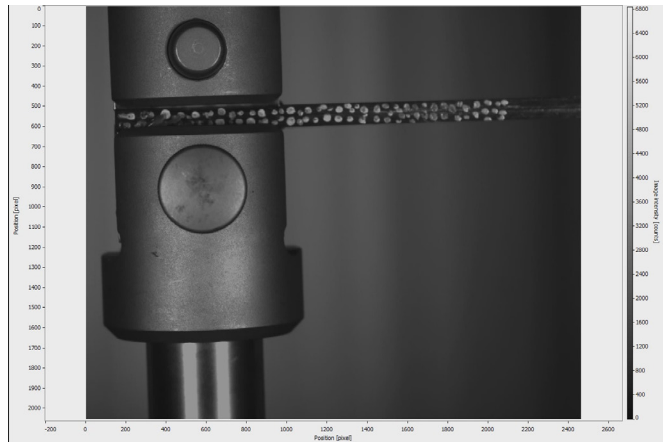

(a)

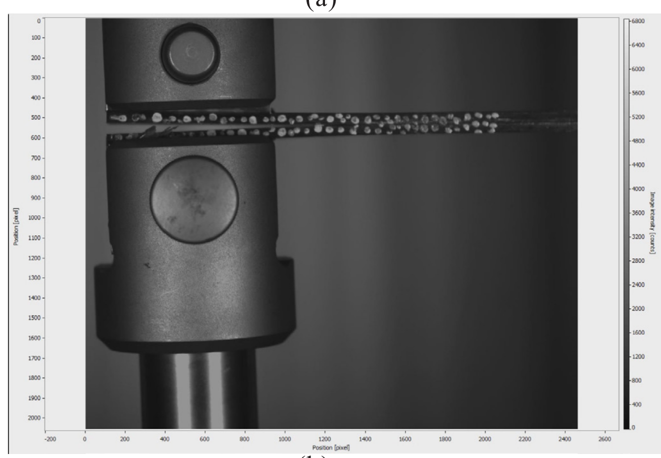

(b)

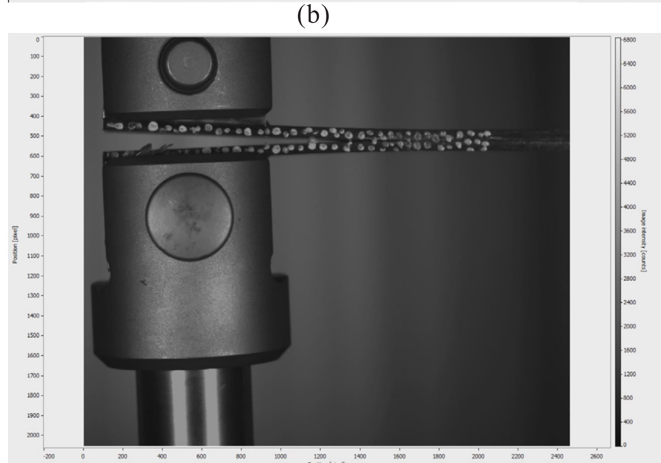

(c)

Figure 13. Experiment during (a) Initial stage; (b) Somewhere in the middle; and (c) At the end.

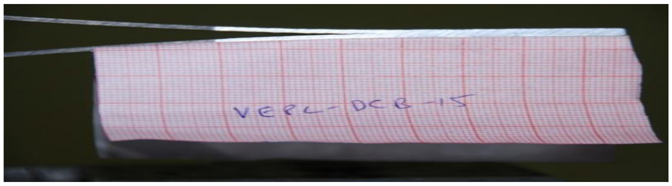

Figure 14. Experimental value was evaluated.

Laminate after carried out test for 0/30° having 70 mm initial crack length was shown in Fig. 14.

5.2 Test Results And Discussion

Table 6 gives the experimentally determined G1C values. As shown in Table 6, we found that the first Pc value obtained during the experiment continued to increase as the layer following angle increased, reaching a maximum value at 0/45°, and then began to decrease, as analyzed by FEM as predicted. However, the G1C value decreases with increasing initial crack length and reaches the maximum value when a0 is 70 mm.

The difference between G1C based on numerical simulations and experimental simulations is less than 10%. Theoretical laminates for comparison with the proposed G1C were calculated under the same initial conditions as the experiments. Gain insights into laminate G1C values based on physical modeling results.

6. CONCLUSIONS

In this study, the delamination effect of LCC was investigated using a combination of experimental results and finite element models. Stratified FEM analysis was performed on 16 bidirectional samples. All samples were prepared following the same orientation as for FEM analysis. For different layer sequences and initial crack lengths, changes in load and displacement are observed and further G1C values are calculated. The force required to fracture the sample was found to depend on the initial crack length and layer orientation. Testing was conducted in accordance with ASTM standard D6671/D6671M-06.

Based on the above study, the following points were noted: -

- Finite element analysis showed that the sample exhibited a steep linear increase in the applied force-displacement curve until a certain threshold was reached, beyond which sudden failure occurred, resulting in a nonlinear decrease in the applied force.
- Different failure modes of laminates under different conditions are analyzed. The study found that as the angle between the laminates increases, the peak force value required to fail increases to 30° (i.e., the angle between the laminates is 30°) and then decreases, and this decrease occurs in shorter The length of the initial crack is important for the calculation of G1C.
- Likewise, increasing the initial crack length will result in less force required to failure, but will also result in larger displacements, thus affecting the determination of the effective G1C value.
- Further improvement in FEM results may be obtained by considering factors such as fibre bridging, delayed failure due to off-axis plies, inaccurate crack length measurement, etc.

REFERENCES

1. Abramovich, H. Introduction to composite materials. Stability and vibrations of thin walled composite structures*,* Woodhead Publishing, 2017, pp. 1-47.

Table 6. Experimental evaluated value of G1C

Angle	a_o (mm)	Pc (N) (Max)	G1C using beam theory (J/m^2) (Avg)	G1C using modified beam theory (J/m^2) (Avg)	G1C using compliance calibration method (J/m^2) (Avg)	G1C using modified compliance calibration method (J/m^2) (Avg)
0/0	70	112.616	1320.45	1340.20	1334.44	1327.27
	80	81.966	830.38	838.75	830.967	836.83
	90	76.53	1022.18	1016.36	1017.10	1022.99
	100	72.24	878.09	871.38	881.10	881.30
	110	63.69	821.03	810.01	805.89	808.11
0/30	70	167.96	1915.78	1914.99	1899.72	1888.73
	80	118.52	1808.37	1812.19	1793.09	1840.41
	90	83.17	1323.60	1321.02	1312.80	1227.75
	100	73.21	996.55	994.43	999.90	988.75
	110	72.14	1018.08	1000.73	1009.93	1014.722
0/45	70	117.43	1721.85	1702.06	1681.30	1707.97
	80	114.51	1789.25	1810.90	1790.07	1800.27
	90	113.95	2012.03	2021.94	2015.70	2020.04
	100	99.54	1656.77	1643.08	1679.94	1669.17
0/60	70	100.25	1744.69	1767.64	1770.41	1768.67
	80	87.37	1804.79	1794.10	1782.91	1780.61

doi: 10.5772/intechopen.91285

2. Khayal, O.M.E.S. A review study of delamination in composite laminated plates, 2019. doi: 10.13140/RG.2.2.12740.07041
3. Jia, R.; Zhao, L.; Curti, R. & Gong, X. Determination of pure mode-I fracture toughness of multidirectional composite DCB specimens. *Engin. Fracture Mech.*, 2021, **252**, 107776.
4. Liu, C.; Bai, R.; Lei, Z.; Di, J.; Dong, D.; Gao, T. & Yan, C. Study on mode-I fracture toughness of composite laminates with curved plies applied by automated fibre placement. *Materials & Design*, 2020, **195**, 108963. doi: 10.1016/j.matdes.2020.108963
5. Gong, Y.; Hou, Y.; Zhao, L.; Li, W.; Zhang, J. & Hu, N. A modified mode I cohesive zone model for the delamination growth in DCB laminates with the effect of fibre bridging. *Int. J. Mech. Sci.*, 2020, **176**, 105514.
6. Teimouri, F.; Heidari-Rarani, M. & Aboutalebi, F.H. An XFEM-VCCT coupled approach for modeling mode I fatigue delamination in composite laminates under high cycle loading. *Engin. Fracture Mech.*, 2021, **249**, 107760.
7. Sebaey, T.A.; Blanco, N.; Costa, J. & Lopes, C.S. Characterisation of crack propagation in mode I delamination of multidirectional CFRP laminates. *Composites Scie. Technol.*, 2012, **72**(11), 1251-1256.
8. Yu, J.; Zhou, C. & Li, S. Experimental and numerical research on the mode I delamination of looped fabric reinforced laminate. *Composites Part B: Engin.*, 2020, **182**, 107566.
9. Tang, Z.; Zhang, H.; Sun, M. & Zhao, X. Advanced composite materials manufacturing technology. *Materials Scie., Adv. Composite Material.*, 2017. *doi: 10.18063/msacm.v1i1.498*
10. Cross, J.O.; Opila, R.L.; Boyd, I.W. & Kaufmann, E.N. Materials characterization and the evolution of materials. *MRS Bulletin*, 2015, **40**(12), 1019-1034. doi: 10.1557/mrs.2015.271
11. Ipek, G.; Arman, Y. & Celik, A. The effect of delamination size and location to buckling behavior of composite materials. *Composites Part B: Engin.*, 2018, **155**, 69-76. doi: 10.1016/j.compositesb.2018.08.009

CONTRIBUTORS

Mr Narendra Kumar Shrivastava completed his BE (Mechanical Engineering) from GEC (NIT) Raipur. He is presently working as a Scientist in DRDO-ASL, Hyderabad. His areas of interest include: Polymeric composite materials and processes, solid propulsion, and projects.
His contribution to the current study includes conceptualisation, planning of experiments, carrying out experiments, test results, analysis and conclusion.

Dr V. Suresh Babu is presently working as a professor & H.O.D. at MED, NIT Warangal. His research interests include: Machine design and strength of material.
In this current study he has given valuable suggestions. supervision, guidance for writing this manuscript, and finalizing the methodology.

Dr Manoj Kumar Buragohain obtained PhD from IIT, Chennai. He is presently working as a Scientist 'G' in DRDO-ASL, Hyderabad. His areas of research include: Design, development, and production of composite products & technology. His main contribution in developing large composite pressure vessels.
In the current study he has given valuable suggestions in conducting the experiments, and supervision. guidance for writing this manuscript and basic

Mr Pushpam Dayal obtained his BE degree in Mechanical engineering from Panjab University, Chandigarh. He is presently working in DRDO-ASL, Hyderabad. His research interests include: Composite materials, aerospace mechanisms, propulsion, systems engineering, and project management.
In the current study he conceptualised, FEM analysis, and carried out experiments, evaluating test results and analysis, and writing the manuscript.